Structure of curved crystals in the thermodynamic limit and the perfect screening condition

Alex Travesset

Phys. Rev. E **94**, 063001 — Published 13 December 2016

DOI: 10.1103/PhysRevE.94.063001

The Structure of Curved Crystals in the Thermodynamic Limit and the Perfect Screening Condition

Alex Travesset*
Department of Physics and Astronomy, Iowa State University, Ames IA 50014

The dislocation and disclination density defining the structure of a crystal constrained on a general curved background is computed analytically in the thermodynamic limit, when the number of particles is arbitrarily large. It is shown that the minimum of the elastic energy, where strains are optimally close to zero, can be formulated in terms of a connection (a rule on how to parallel transport vectors). It is shown that the thermodynamic solution consist of disclinations surrounded by scars (grain boundaries with variable spacing). The approach allows to compute the interaction potential. For a sphere, a full characterization of the scars is provided, and it is shown that the potential of interaction among disclinations "dressed" by scars is inversely proportional to the sinus of the geodesic distance and that the ground state consists of twelve dressed disclinations that display icosahedral symmetry. The case of a torus is also considered. More generally, the thermodynamic solution implements a "perfect screening" condition, where defects completely screen the Gaussian curvature. Implications for the problem of melting are discussed.

I. INTRODUCTION

Understanding the type of crystalline order that occurs on a lattice constrained on a general curved manifold is a fundamental problem with many recent experimental realizations in soft systems such as lipids, colloids or surfactants[1–7] as well as in hard systems such as metallic glasses, superconductors or carbon nanotubes among many other relevant examples[8]. Although there has been remarkable theoretical progress [9–22], most studies have focused on the limit of a relatively small number of particles. In this article, I investigate the thermodynamic limit, that is, the limit when the number of particles is arbitrarily large. This situation has been addressed previously[3, 20, 23] by considering a limit of weak curvature.

The key elements in any crystal on a curved background are topological defects and Riemannian curvature[24, 25]. Indeed, disclinations and dislocations are necessary to relieve the stresses induced by the curvature. Intuitively, the disclinations are akin to electrostatic charges and the dislocations to polarizable dipoles, which combine to neutralize the curvature. In two dimensional solids, for example, previous calculations strongly suggest [3, 11, 20] that in the thermodynamic limit, at zero temperature, a "perfect" screening of defects neutralizing the curvature should follow. More precisely

$$\int K(\mathbf{x})dA = \sum_{i=1}^{N_D} q_i + \int \nabla\cdot\vec{P}dA\ , \qquad (1)$$

with $K(\mathbf{x})$ the Gaussian curvature, N_D is the number of isolated disclinations (each of charge q_i) and $\vec{P}$ is the "polarization", which is related to the dislocation density.

A clear example of "perfect screening" is provided by an icosahedron, see Fig. 1, where each vertex accumulates a $\frac{\pi}{3}$ of Gaussian curvature, which are screened by

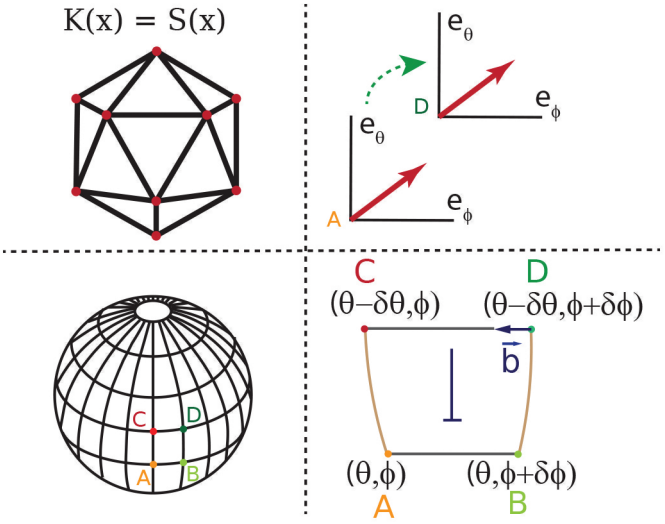

FIG. 1. (Top Left) Icosahedron, where each vertex is a disclination with Gaussian curvature $K(\mathbf{x}) = \frac{\pi}{3}\delta(\mathbf{x}-\mathbf{x}_i)$.(Top Right) Trivial parallel transport from point A to D by the vector fields e_θ, e_ψ. (Bottom Left) Frame corresponding to the trivial connection with the vortices at the north and south poles. (Bottom Right) Parallel transporting segment AC along segment AB, and parallel transporting segment AB along AC results in gap that is given by $\vec{b} = -\cot(\theta)e_\psi$, indicative of a non-zero torsion or dislocation density.

$\frac{\pi}{3}$ disclinations. In this case, however, no additional dislocations are required and the remaining lattice, consisting of six coordinated vertices forming a perfectly planar hexagonal lattice, can be constructed on the planar face of the icosahedron. Note that the physical bonds between nearest neighbor particles in different sites are parallel. On a general manifold, however, the curvature is continuous, and, in principle, cannot be completely screened by a number of discrete disclination charges. In such case, there is no notion of parallelism, as attempting to construct the lattice requires the specification of a rule that tells how to parallel transport vectors (a connection). In

* trvsst@ameslab.gov

curved geometries, parallel transport of a vector generally depends on the amount of curvature encircled by the path, so the parallel transport is not unique, and not suitable for the construction of a lattice. It is known, however, that a path independent parallel transport from a point P_1 to any other point P_2 (on a sphere, for example) can be defined from

$$\vec{V} = V^\theta e_\theta(P_1) + V^\psi e_\psi(P_1) \to V^\theta e_\theta(P_2) + V^\psi e_\psi(P_2) \ , \tag{2}$$

where e_θ, e_ψ are the unit tangent vectors defined by spherical coordinates. As shown in Fig. 1, such parallel transport has two distinct features: It is singular at the north and south poles, and the parallel transport of two vectors along each other does not result in a closed parallelogram, as shown in Fig. 1. The first feature is indicative that the entire Gaussian curvature is now localized at both poles in the form of two vortices each with charge 2π. The second is that this newly defined connection has geometric torsion[26]. Such "trivial" connections have been known, for example in navigation, as they correspond to loxodromic paths, which become straight lines in the Mercator projection. In physical terms, such connections implement a lattice where the rows of atoms are as close as possible to have zero strains. This equivalence between optimal strains and trivial connections forms the basis of the approach developed in this paper.

II. GEOMETRIC FORMULATION FOR CRYSTALS IN ARBITRARY GEOMETRIES

While disclinations are associated with Gaussian curvature, dislocations are identified as sources of geometric torsion[24, 27]. In this way, a very natural physical interpretation of the process of "trivialization" of a connection by torsion emerges, where the dislocations role is to "spread" the discrete disclination charge and fully screen out the curvature, resulting in a configuration that is basically flat, and where the parallel transport is defined by the vectors defining the crystallographic axis. This is a completely general result, beyond consideration of crystals. For example, the free energy of an hexatic membrane with bond orientational order θ on a curved manifold with metric $g_{\mu\nu}$ is given as[28]

$$F_{hex} = \frac{K_A}{2}\int d^2\mathbf{x}\sqrt{g}g^{\mu\nu}(\partial_\mu\theta+\Omega^D_\mu-\Omega^L_\mu)(\partial_\nu\theta+\Omega^D_\nu-\Omega^L_\nu) \ , \tag{3}$$

where $\nabla_\mu = \frac{\partial}{\partial x^\mu} - \Omega^L_\mu$ defines the standard covariant derivative (Levi-Civita) connection and Ω^D accounts for the distribution of disclinations. The difference in sign reflects that defects screen curvature of the same sign. It is convenient to consider $\Omega^{D,L}$ as 1-forms, whose exterior derivative d[26] gives

$$d\Omega^L = K(\mathbf{x})\Omega_M \ , \ d\Omega^D = S^D(\mathbf{x})\Omega_M \ , \tag{4}$$

with $K(\mathbf{x})$ the Gaussian curvature, $S^D(\mathbf{x}) = \sum_{j=1}^{N_D}\frac{q_j}{\sqrt{g}}\delta(\mathbf{x}-\mathbf{x}^j)$ is the disclination density (with q_i the disclination charge) and $\Omega_M = \theta^1\wedge\theta^2 = \sqrt{g}dx^1\wedge dx^2$ is the volume two form.

Thus, the free energy becomes a function of the combination $\Upsilon_\mu = \Omega^D_\mu - \Omega^L_\mu$ and is given by

$$F = \frac{Y}{2}(d\Upsilon, \frac{1}{\Delta^p}d\Upsilon) = \int\int (K^D - S)\frac{1}{\Delta^p}(K^D - S) \ , \tag{5}$$

where Δ is the Laplacian. The case $p = 1$ describes the hexatic order Eq. 3[28] while $p = 2$ describes a general 2D crystal[11]. For this latter case, dislocations need to be introduced as

$$\Omega^{(D,d)}_\mu = \Omega^D_\mu + \sum_{i=1}^{N_d}\frac{b^i_\mu}{\sqrt{g}}\delta(\mathbf{x}-\mathbf{x}^i) \tag{6}$$

$$S^{(D,d)}(\mathbf{x}) = \sum_{i=1}^{N_d}\frac{1}{\sqrt{g}}\epsilon^{\alpha\beta}b^i_\alpha\partial_\mu(e_\beta{}^\mu\delta(\mathbf{x}-\mathbf{x}^i)) + S^D(\mathbf{x})$$

where b_α is the Burgers vector and formulas have been written in local or "einvein" coordinates (see SI). For a flat monolayer, the above formulas reduce to the known results[25].

The thermodynamic limit is obtained as the lattice constant a of the underlying lattice becomes vanishingly small compared with the dimensions (in physical units) of the curved manifold. In such limit, the dislocation density satisfies

$$\sum_{i=1}^{N_d}\frac{b^i_\alpha}{\sqrt{g}}\delta(\mathbf{x}-\mathbf{x}^i) = \beta_\alpha(\mathbf{x}) + \mathcal{O}(a/R) \tag{7}$$

where R is a characteristic parameter defining the surface (For a sphere, R is obviously the radii, for a torus, the smaller of the two radii, etc..). This formula defines a continuum dislocation density β, and the last term serves to remind the error made in such approximation, an issue to which I will return later.

From differential geometry, the standard Levi-Civita connection satisfies $\Omega^{L,\alpha} = -d\theta^\alpha$. A new connection may be defined by subtracting to the Levi Civita connection the dislocation density $\Omega^C_\alpha = \Omega^L_\alpha - \beta_\alpha$, and satisfies

$$d\hat{\theta}^\alpha + \Omega^{C,\alpha}\Omega_M = \beta^\alpha\Omega_M \tag{8}$$

$$d\Omega^C = \mathcal{K}\Omega_M \ , \tag{9}$$

Upon identifying β with the torsion, these equations are the Cartan Structure equations[26], which define the most general connection that is compatible with the metric (see also, appendix 1). Here $\mathcal{K}$ is the curvature associated with this new connection, which is different than the Gaussian curvature. Following the trivialization discussed in Fig. 1, the dislocation density (the torsion) β will be chosen so that the new curvature $\mathcal{K}$ is given as

$$\mathcal{K}(\mathbf{x}) = \sum_{i=1}^{D}\frac{q_j}{\sqrt{g}}\delta(\mathbf{x}-\mathbf{x}_i) \to d\Upsilon = 0 \ , \tag{10}$$

that is, the curvature is entirely concentrated in a few isolated points (such as the two poles for the case in Fig. 1).

As I will argue further below, such construction is always possible. In this way, the dislocation density β succeeds in undressing the Gaussian curvature into isolated charges, which are perfectly screened by disclinations, in the same way as for the icosahedron previously discussed. In this way, the trivialization of the connection implements the "perfect screening" condition.

Thus, the equations defining the minimum of the free energy Eq. 5, that is Eq. 10, amounts to the statement that Υ is a closed 1-form and that the dislocation density is determined up to an arbitrary exact form

$$\begin{aligned} d\Upsilon &= 0 \\ \beta' &= \beta + d\zeta \end{aligned} \tag{11}$$

so that the solution Eq. 10 is not unique. In addition, if the de Rham cohomology group $\mathrm{H}^1(\mathrm{S})$ of the manifold is non-trivial, additional topological inequivalent solutions become possible.

Note that the Stokes theorem implies that the integral over the entire closed manifold of the form in Eq. 11 is

$$\int d\zeta = 0 \ , \tag{12}$$

so that the additional "gauge invariance" is interpreted as modifying the distribution of dislocations, but not its total number.

III. RESULTS: THE CASES OF THE SPHERE AND THE TORUS.

As a first example, I consider the manifold to be a sphere S^2, described with coordinates (ϑ, ψ). The Levi-Civita connection is

$$\Omega_L = -\cot(\vartheta)\hat{\theta}^{\psi} \tag{13}$$

so that $d\Omega^L = 1 \cdot \Omega_M$ and the Gaussian curvature is $K = 1$.

The obvious dislocation density calculated from the Cartan structure equations Eq. 8 is $\beta_\vartheta = 0, \beta_\psi = -\cot(\vartheta)$, which exactly implements the "Mercator" trivialization discussed in the introduction. The associated curvature becomes

$$\mathcal{K} = 2\pi\delta(\vartheta - 0) + 2\pi\delta(\vartheta - \pi) \ , \tag{14}$$

that is, as expected, the entire curvature is concentrated into two vortices, each carrying a 2π curvature. Such defects are not consistent with a spherical crystal. An acceptable solution containing twelve $q = \frac{\pi}{3}$ disclinations can be found as a superpositions of 6 of these solutions, namely

$$\begin{aligned} \beta^{\vartheta} &= -\frac{1}{6}\sum_{i=1}^{6} \frac{\cot(\omega_i)}{\sin(\omega_i)} \sin(\vartheta_i)\sin(\psi - \psi_i) \\ \beta^{\psi} &= \frac{1}{6}\sum_{i=1}^{6} \frac{\cot(\omega_i)}{\sin(\omega_i)} \left[\sin(\vartheta)\cos(\vartheta_i) - \right. \\ &\quad \left. - \cos(\vartheta)\sin(\vartheta_i)\cos(\psi - \psi_i)\right] \end{aligned} \tag{15}$$

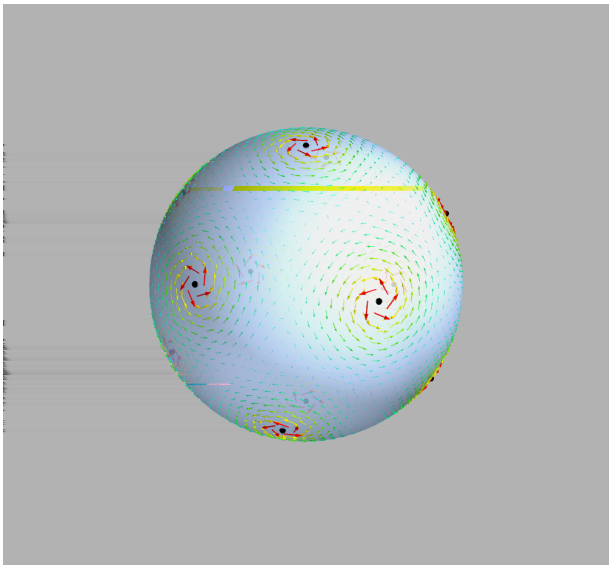

FIG. 2. Solution for the dislocation density on the sphere in the thermodynamic limit (Eq. 15 and Eq. 19). Solution Eq. 15

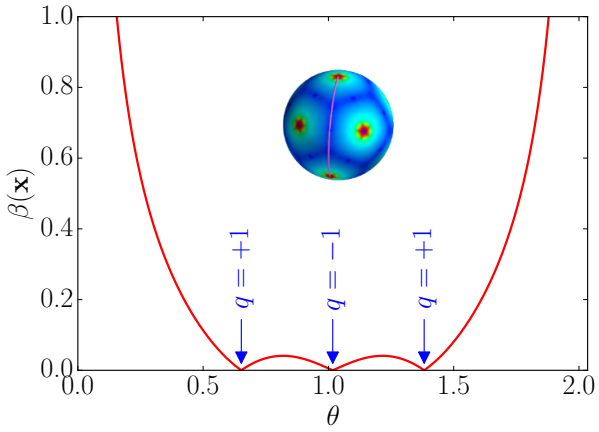

FIG. 3. Magnitude of the dislocation density as a function of geodesic distance from one disclination to the next-to-nearest disclination. The three zeros correspond to two vortices $q = 1$ and one anti-vortex $q = -1$. The magnitude diverges near disclinations.

where $(\vartheta_i, \varphi_i)_{i=1\cdots6}$ describes the orientations of the axis where each of the six disclination pairs are placed and $\cos(\omega_i) = \cos(\vartheta)\cos(\vartheta_i) + \sin(\vartheta)\sin(\vartheta_i)\cos(\psi - \psi_i)$. Since one disclination pair can be placed along the axis defining the north-south pole $\vartheta = 0$, and another disclination can be placed at $\psi = 0$, the solution Eq. 15 has nine free parameters.

There is, however, an additional boundary condition that must be met. In its most general case, Eq. 15 leads to a situation where Burgers vector add to non-zero values at the position of disclinations. This is clearly unphysical as a disclination cannot have a Burgers vector. The same conclusion can also be arrived from Eq. 7, as, by construction, each of the discrete dislocation density

at finite lattice spacing will obviously have a zero Burgers vectors at the disclination, so this should be also be the case for the limit. Therefore, I arrive at the following boundary condition

$$\begin{aligned}\beta^{\vartheta}(\mathbf{x}_j) &\tilde{=} 0 \\ \beta^{\psi}(\mathbf{x}_j) &\tilde{=} 0 \ ,\end{aligned} \tag{16}$$

where $\mathbf{x}_j, j = 1 \cdots 6$ runs over the positions of each disclination pair, and the $\tilde{=}$ sign is used to emphasize that the actual disclination at $\mathbf{x}_j$ is should be omitted.

The general potential between two dressed disclinations, that is, including the scars, is a function of the geodesic distance s, so it can be written as $V(s)$. The overall potential for the twelve dressed disclinations will therefore be

$$U = \sum_{i=1}^{12} \sum_{j>i}^{12} V(s_{ij}) \ , \tag{17}$$

where s_{ij} is the geodesic distance between the two i, j disclinations. Note, that the minimization of the above potential energy should lead to Eq. 15 and Eq. 16. Such condition immediately leads to $V(s) = \frac{1}{\sin(s)}$ as the only possibility for function V (this statement can be verified by showing that the minimum of Eq. 18 leads to Eq. 15 and Eq. 16). Note that the interaction between a pair of dressed disclinations is always repulsive. Therefore, the potential energy for the twelve disclinations is given as

$$U = \sum_{i=1}^{6} \sum_{j>i}^{6} \frac{1}{\sin(s_{ij})} \ , \tag{18}$$

where the summation only needs to run up to 6, as the other 6 dressed disclinations follow by inversion symmetry. Thus, Eq. 16 appears as the condition of zero force between screened disclinations.

Given that the potential Eq. 18 implies that a disclination pair repeal each other, it is intuitively clear, and I have also verified it with numerical minimizations, that the zero force condition Eq. 16 consists of 12 disclinations that sit on the vertices of an icosahedron, in positions

$$(0,0), (\arctan(2), \frac{2\pi}{5}k), (\pi - \arctan(2), \frac{\pi}{5} + \frac{2\pi}{5}k), (\pi, 0) \ , \tag{19}$$

with $k = 0 \cdots 4$. Note that even though $d\Upsilon = 0$, the form Υ itself is not zero. Also, for a sphere $\mathrm{H}^1(S^2) = 0$, and there are not additional topological distinct solutions.

The dislocation density β defined by Eq. 15 and Eq. 19 is shown in Fig. 2. Note that β can be regarded as a vector field, so it displays 32 vortices (12 around each disclination) and 30 anti-vortices (mid-way each nearest-neighbor disclinations). The magnitude of the dislocation density is shown in Fig. 3 along the path connecting two next-to-nearest disclination, where it intersects three vortices (2 vortices and 1 antivortex). The additional "gauge" invariance can be used to optimize the distribution Eq. 15: by including a function $\zeta(\psi) = a\cos(5\psi)$ (on each of the 12 disclinations), the dislocations become

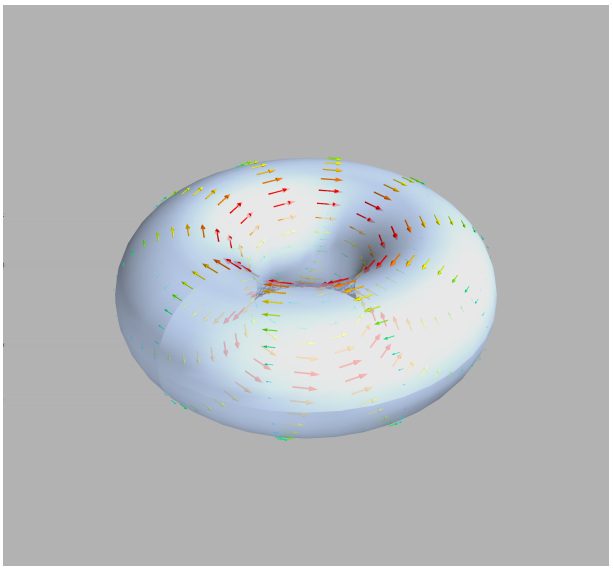

FIG. 4. Solution for the dislocation density on the torus in the thermodynamic Eq. 20 for aspect ratio $r = 1.7$. Solution with $\lambda_1, \lambda_2, \zeta_1, \zeta_2 = 0$.

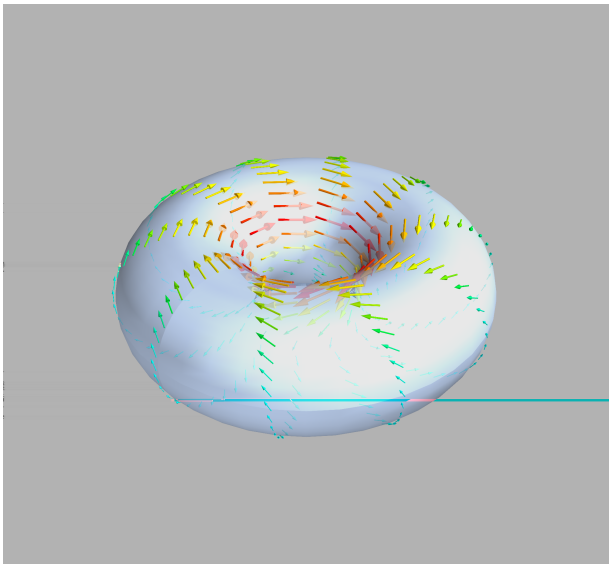

FIG. 5. Solution for the dislocation density on the torus in the thermodynamic Eq. 20 for aspect ratio $r = 1.7$. Solution with $\lambda_1 = 0.5, \lambda_2 = 0.3$

significantly different from zero only along the paths connecting nearest neighbor disclinations defining a distribution of "pentagonal buttons"[11].

The same methods provide the solution for a torus manifold. Using (ϑ, α) coordinates (see appendix Sect 2, the Levi Civita connection is $\Omega^L = -\frac{\sin(\alpha)}{r+\cos(\alpha)}\theta^1$, where $r = \frac{R_1}{R_2} > 1$ is the aspect ratio of the torus. The most general dislocation density satisfying Eq. 11 is

$$\beta = -\sin(\alpha)d\vartheta + \lambda_1 d\vartheta + \lambda_2 d\alpha + d(\zeta_1(\alpha) + \zeta_2(\vartheta)) \ , \tag{20}$$

where λ_1, λ_2 are arbitrary real numbers that parameterize the De Rahm Cohomology group $H^1(T^2) = R \oplus R$

and $\zeta_{1,2}$ are arbitrary functions. In Fig. 5(top), the solution with $\lambda_1, \lambda_2, \zeta_1, \zeta_2 = 0$ is shown, and consists of finite length grain boundaries with no disclinations (pleats[3]). In Fig. 5(bottom), the solution with ($\lambda_1 = 0.5, \lambda_2 = 0.3$) is shown, with Burgers vectors that twist along the circles with constant ϑ. Solutions with isolated disclinations[8] are also possible, but will not be discussed here.

IV. CONCLUSIONS

The general solution Eq. 11 immediately leads to a free energy Eq. 5 that is identically zero. This does not imply that the resulting crystal is perfectly flat, it is only flat up to corrections of order $\mathcal{O}(a/R)$, see Eq. 7. A concrete example will serve to illustrate this degeneracy: The energy of an isolated disclination in a flat disc of radius R grows like R^2[25]. Whenever such disclination is surrounded by low angle grain boundaries, the "perfect screening" condition leads to an elastic energy that is of order $R^2\mathcal{O}(a/R) = aR$. There is, however, a large freedom in the choice of the actual grain boundaries: m radial grains where dislocations within a grain are separated a distance

$$D = b/\left(2\sin\left[\frac{\pi}{6m}\right]\right) \tag{21}$$

will perfectly screen the disclination for any value of m or orientation of the grains[14]. This freedom in the choice of grain boundary is what the "gauge symmetry" Eq. 11, in the general case, parameterizes.

Of course, the degeneracy implied by the "gauge symmetry" is removed at order $\mathcal{O}(a/R)$, but then, there are additional free energy contributions that come into play, such as, defect core energies, bond orientational terms and many others. The critical step is therefore the continuum limit Eq. 7. This limit can be performed by the following construction[15]: The minimum number of disclinations is determined by topological constraints and placed where the curvature is maximum. Dislocations defining the scar are then added whenever the area around that point exceeds or fails the area of an entire triangle $= \sqrt{3}a^2/4$, where a is the lattice constant. Such dislocation density will provide an optimal approximation for finite a and converges to the exact analytical solution.

Although it may appear that the results have been obtained within linear elastic theory, they are, in fact more general. From standard results in differential geometry[26], it is possible to express $\Upsilon = d^\dagger(\Psi\Omega_M)$, where Ψ is the generalization of the Airy function[25] to curved geometries. Such function satisfies an expansion in the "incompatible stress function", which goes beyond linear elasticity theory [29]. This formalism provides a rigorous justification for the formalism discussed here, but making it more precise will be left for a subsequent publication.

In summary, an explicit solution of the structure, in the form of the distribution of disclinations and dislocations in the thermodynamic limit for *any* geometry is provided. The solution is highly degenerate. The results provide a precise and practical formulation of the perfect screening condition [3, 11, 20] and allow a determination of the effective potential between disclinations dressed with scars, Eq. 18. Using these results, it is shown that in the thermodynamic limit, the ground state of a sphere contains 12 disclinations with the symmetry of an icosahedron. With the current advances of both experimental and numerical methods [18, 21, 22], where large systems are realized, the importance of the thermodynamic limit result becomes even more clear. Furthermore, the underlying geometric interpretation is completely revealed.

The discussion in this paper has been confined to closed manifolds. It is possible to generalize the results to manifolds with boundaries. If it is allowed to adjust the boundary so that the stresses are zero at the boundary, the equations defining the perfect screening Eq. 13 can be applied with the only modification that the dislocation density is zero at the boundary. If some stress is applied at the boundaries, as considered in ref. [20, 23], these external stresses need to be implemented as boundary conditions, which is not conceptually difficult but somewhat more complex in practice[29].

The results presented are also relevant for a discussion of finite temperature effects. For a sphere, for example, it shows that the icosahedral order of the disclinations is maintained in the thermodynamic limit, and therefore, the long-range effect of such disclinations, which interact with a potential Eq. 18, keeps the icosahedral symmetry all the way till melting[25]. The precise melting mechanism will be investigated in future work. Last, but not least, the solutions discussed in this paper are relevant for other problems, for example, in determining triangulations of a manifold where triangles are optimally close to equilateral.

ACKNOWLEDGMENTS

I acknowledge many discussions with M. Bowick, P. Chaikin, R. Guerra and C. Patrick. This work is supported by the National Science Foundation project DMR-CMMT 1606336 CDSE: Design Principles for Ordering Nanoparticles into Super-crystal.

1. Differential Geometry basics

A general surface is described by an embedding $\vec{r}(\mathbf{x})$, and inherits a metric from flat space given by

$$g_{\mu\nu} = \partial_\mu \vec{r} \cdot \partial_\nu \vec{r}\,. \tag{22}$$

It is convenient to diagonalize the metric in terms of the non-coordinate basis $\{\hat{e}_\alpha\}$ and $\{\hat{\theta}^\alpha\}$, through the vielbeins coefficients

$$\hat{\theta}^\alpha = e^\alpha{}_\mu dx^\mu \quad , \quad \hat{e}_\alpha = e_\alpha{}^\mu \frac{\partial}{\partial x_u}\,, \tag{23}$$

so that $g_{\mu\nu} = \delta_{\alpha\beta} e^{\alpha}{}_{\mu} e^{\beta}{}_{\nu}$. The 1-form connection describes how to transport vectors at different points, and is defined according to

$$\omega^{\alpha}{}_{\beta} = \Gamma^{\alpha}{}_{\gamma\beta} \hat{\theta}^{\gamma} \ , \tag{24}$$

where the tensor $\Gamma^{\alpha}{}_{\gamma\beta}$ implements the connection. The connection must be compatible with the metric, so that the norm and angle of two vectors does not change during parallel transport. This metric compatibility condition leads to

$$\omega_{\alpha\beta} = -\omega_{\beta\alpha} \Longrightarrow \omega_{\alpha\beta} = \varepsilon_{\alpha\beta} \Omega \ , \tag{25}$$

where herein the right arrow is used to indicate the simplifications that occur for the two dimensional case. Here $\Omega = \Omega_{\alpha} \hat{\theta}^{\alpha}$ is a 1-form. With these definitions, the Cartan structure equations are given as

$$\begin{aligned} d\hat{\theta}^{\alpha} + \omega^{\alpha}{}_{\beta} \wedge \hat{\theta}^{\beta} = T^{\alpha} \Longrightarrow d\hat{\theta}^{\alpha} + \Omega^{\alpha} \Omega_M = \mathcal{B}^{\alpha} \Omega_M \\ d\omega^{\alpha}{}_{\beta} + \omega^{\alpha}{}_{\gamma} \wedge \omega^{\gamma}{}_{\beta} = R^{\alpha}{}_{\beta} \Longrightarrow d\Omega = \mathcal{K} \Omega_M \ , \end{aligned} \tag{26}$$

where $T^{\alpha} = \frac{1}{2} T^{\alpha}{}_{\beta\gamma} \hat{\theta}^{\beta} \wedge \hat{\theta}^{\gamma} \Longrightarrow \mathcal{B}^{\alpha} \Omega_M$ is the torsion tensor, and $R^{\alpha}{}_{\beta} = \frac{1}{2} R^{\alpha}{}_{\beta\gamma\delta} \hat{\theta}^{\gamma} \wedge \hat{\theta}^{\delta} \Longrightarrow \varepsilon^{\alpha}{}_{\beta} \mathcal{K} \Omega_M$ is the curvature tensor, with $\Omega_M = \hat{\theta}^1 \wedge \hat{\theta}^2$ the area form.

There is a special connection, sometimes named the Levi-Civita (LC) connection, where the torsion vanishes identically. In this case, vectors are parallel transported along geodesics. I denote this connection as Ω^L, and it satisfies the equations.

$$\begin{aligned} \Omega^{L,\alpha} \Omega_M = -d\hat{\theta}^{\alpha} \\ d\Omega^L = K \Omega_M \ , \end{aligned} \tag{27}$$

where $K(\mathbf{x})$ is the standard Gaussian curvature.

2. Toroidal Coordinates

The toroidal coordinates employed in this paper are:

$$\begin{aligned} x(\alpha, \vartheta) &= (R_1 + R_2 \cos(\alpha)) \cos(\vartheta) \\ y(\alpha, \vartheta) &= (R_1 + R_2 \cos(\alpha)) \sin(\vartheta) \\ z(\alpha, \vartheta) &= R_2 \sin(\alpha) \ , \end{aligned} \tag{28}$$

where both α, ϑ run from 0 to 2π.

[1] A. R. Bausch, M. J. Bowick, A. Cacciuto, A. D. Dinsmore, M. F. Hsu, D. R. Nelson, M. G. Nikolaides, A. Travesset and D. A. Weitz, *Science*, 2003, **299**, 1716–1718.

[2] M. Dubois, V. Lizunov, A. Meister, T. Gulik-Krzywicki, J. M. Verbavatz, E. Perez, J. Zimmerberg and T. Zemb, *Proceedings of the National Academy of Sciences of the United States of America*, 2004, **101**, 15082–15087.

[3] W. T. M. Irvine, V. Vitelli and P. M. Chaikin, *Nature*, 2010, **468**, 947–951.

[4] W. T. M. Irvine, A. D. Hollingsworth, D. G. Grier and P. M. Chaikin, *Proceedings of the National Academy of Sciences*, 2013, **110**, 15544–15548.

[5] E. A. Matsumoto, D. A. Vega, A. D. Pezzutti, N. A. Garca, P. M. Chaikin and R. A. Register, *Proceedings of the National Academy of Sciences*, 2015, **112**, 12639–12644.

[6] M. Brojan, D. Terwagne, R. Lagrange and P. M. Reis, *Proceedings of the National Academy of Sciences*, 2015, **112**, 14–19.

[7] S. Guttman, Z. Sapir, M. Schultz, A. V. Butenko, B. M. Ocko, M. Deutsch and E. Sloutskin, *Proceedings of the National Academy of Sciences*, 2016, **113**, 493–496.

[8] M. J. Bowick and L. Giomi, *Advances in Physics*, 2009, **58**, 449–563.

[9] H. S. Seung and D. R. Nelson, *Phys. Rev. A*, 1988, **38**, 1005–1018.

[10] A. Pérez-Garrido, M. J. W. Dodgson and M. A. Moore, *Phys. Rev. B*, 1997, **56**, 3640–3643.

[11] M. J. Bowick, D. R. Nelson and A. Travesset, *Physical Review B*, 2000, **62**, 8738–8751.

[12] M. Bowick, A. Cacciuto, D. R. Nelson and A. Travesset, *Physical Review Letters*, 2002, **89**, 185502–185505.

[13] M. Bowick, D. R. Nelson and A. Travesset, *Physical Review E (Statistical, Nonlinear, and Soft Matter Physics)*, 2004, **69**, 041102–12.

[14] A. Travesset, *Physical Review B (Condensed Matter and Materials Physics)*, 2003, **68**, 115421–15.

[15] A. Travesset, *Physical Review E (Statistical, Nonlinear, and Soft Matter Physics)*, 2005, **72**, 036110–8.

[16] V. Vitelli, J. B. Lucks and D. R. Nelson, *Proceedings of the National Academy of Sciences*, 2006, **103**, 12323–12328.

[17] G. Vernizzi, R. Sknepnek and M. Olvera de la Cruz, *Proceedings of the National Academy of Sciences*, 2011, **108**, 4292–4296.

[18] H. Kusumaatmaja and D. J. Wales, *Phys. Rev. Lett.*, 2013, **110**, 165502.

[19] Z. Yao and M. O. de la Cruz, *Phys. Rev. E*, 2013, **87**, 012603.

[20] A. Azadi and G. M. Grason, *Phys. Rev. Lett.*, 2014, **112**, 225502.

[21] C. Negri, A. L. Sellerio, S. Zapperi and M. C. Miguel, *Proceedings of the National Academy of Sciences*, 2015, **112**, 14545–14550.

[22] F. L. Jiménez, N. Stoop, R. Lagrange, J. Dunkel and P. M. Reis, *Phys. Rev. Lett.*, 2016, **116**, 104301.

[23] A. Azadi and G. M. Grason, *Phys. Rev. E*, 2016, **94**, 013003.

[24] J. Sadoc and R. Mosseri, *Geometrical Frustration*, Cambridge University Press, 1999.

[25] D. Nelson, *Defects and Geometry in Condensed Matter Physics*, Cambridge Press, 2002.

[26] M. Nakahara, *Geometry, Topology and Physics*, Adam Hilger, 1990.

[27] M. Bowick and A. Travesset, *J. Phys. A:Math. Gen.*, 2001, **34**, 1535.
[28] F. David, E. Guitter and L. Peliti, *J. Phys.*, 1988, **49**, 2059–2066.
[29] M. Moshe, E. Sharon and R. Kupferman, *Phys. Rev. E*, 2015, **92**, 062403.